

AUS Repository

Ultrasonically Controlled Albumin-conjugated Liposomes for Breast Cancer Therapy

Item Type	Peer-Reviewed;Article;Postprint
Authors	Awad, Nahid S.;Paul, Vinod;Al-Sayah, Mohammad;Husseini, Ghaleb
Citation	Nahid S. Awad, Vinod Paul, Mohammad H. Al-Sayah & Ghaleb A. Husseini (2019) Ultrasonically controlled albumin-conjugated liposomes for breast cancer therapy, <i>Artificial Cells, Nanomedicine, and Biotechnology</i> , 47:1, 705-714, DOI:10.1080/21691401.2019.1573175
DOI	10.1080/21691401.2019.1573175
Publisher	Taylor and Francis Online
Download date	2026-06-08 03:11:42
Link to Item	http://hdl.handle.net/11073/16588

Ultrasonically Controlled Albumin-conjugated Liposomes for Breast Cancer Therapy

Nahid Awad^a, Vinod Paul^a, Mohammad H. Al-Sayah^{b,c}, Ghaleb Hussein^{*,a,c}

^a*Department of Chemical Engineering, American University of Sharjah, PO. Box 26666, Sharjah, UAE*

^b*Department of Biology, Chemistry and Environmental Sciences, American University of Sharjah, PO. Box 26666, Sharjah. UAE*

^c*Biosciences & Bioengineering Research Institute, American University of Sharjah, PO. Box 26666, Sharjah. UAE*

*Corresponding author:

Professor of Chemical Engineering and Dana Gas Endowed Chair in Chemical Engineering
Department of Chemical Engineering
American University of Sharjah
Sharjah,
United Arab Emirates
g Hussein@aus.edu

<https://doi.org/10.1080/21691401.2019.1573175>

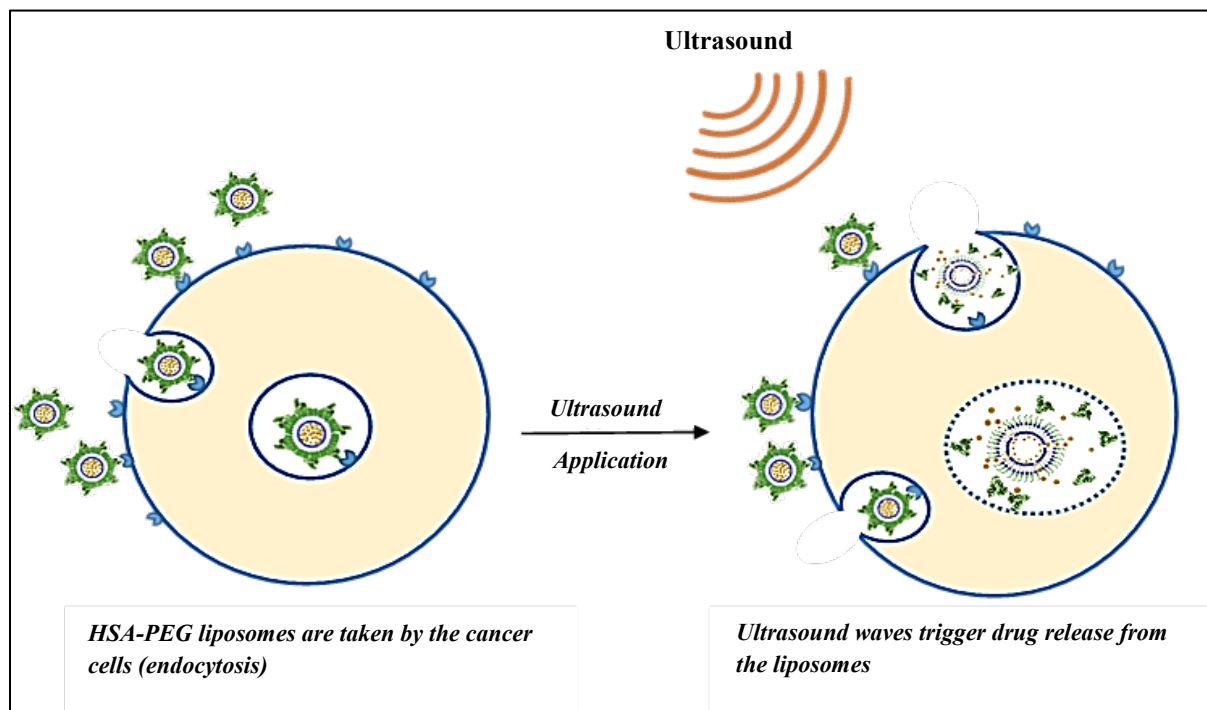
Nahid S. Awad, Vinod Paul, Mohammad H. Al-Sayah & Ghaleb A. Hussein

(2019) Ultrasonically controlled albumin-conjugated liposomes for breast cancer therapy, *Artificial Cells, Nanomedicine, and Biotechnology*, 47:1, 705-714,
DOI:10.1080/21691401.2019.1573175

Ultrasonically Controlled Albumin-conjugated Liposomes for Breast Cancer Treatment

Abstract:

Targeted liposomes have high potentials in the specific and effective delivery of their loaded therapeutic agents to the tumor site. Once at the tumor site, it is important that these liposomes are triggered to release their load in a controlled and effective manner. In this study, pegylated (stealth) liposomes conjugated to human serum albumin (HSA) were investigated for the delivery of a model drug (calcein) to breast cancer cells. The fluorescent results showed that calcein uptake by the two breast cancer cell lines (MDA-MB-231 and MCF-7) was significantly higher with the HSA-PEG liposomes compared to the non-targeted control liposomes. Furthermore, the exposure to low-frequency ultrasound (LFUS) resulted in a statistically significant uptake of calcein compared to the uptake without ultrasound. The described drug delivery (DD) system, which involves combining the targeted liposomal formulation with ultrasonic triggering techniques, promises a safe, effective and site-specific breast cancer therapy.



Keywords: human serum albumin, liposomes, calcein, breast cancer, ultrasound.

1. Introduction

Chemotherapy is an effective method for breast cancer treatment showing many advantages in prolonging patients' survival time. However, the high toxicity of this treatment limits the drug dosage that can be administrated [1]. A promising solution to overcome these unwanted effects is to use smart nanocarriers that are biocompatible, biodegradable and stimuli-responsive. These nanocarriers are able to encapsulate the drugs efficiently. Thus, ensuring the safe delivery of these drugs to the tumor site. When triggered, nanocarriers release their load destroying the cancer cells while limiting the exposure of the healthy cells to these toxic drugs.

Liposomes are nanoparticles composed of phospholipids which self-assemble to form bilayer spherical shapes. These ideal nanocarriers are highly stable and biocompatible with a high encapsulating capacity for both hydrophilic and hydrophobic drugs. In addition, liposomes can be easily modified to increase their circulation time by coating them with polymers such as polyethylene glycol, also known as stealth liposomes [2]. The drugs encapsulated inside these nanocarriers circulate in the body without affecting the healthy tissues due to the inability of these drug delivery vehicles to cross the endothelial barrier. On the other hand, the nanocarriers easily accumulate and are retained at the tumor site by penetrating through the leaky blood vessels formed as a result of the aberrant angiogenesis in tumors [3]. This is known as the “enhanced permeability and retention effect” (EPR) which is the mechanism behind the “passive targeting” of tumor tissues [4, 5]. “Active targeting” of specific receptors on the surfaces of the tumor cells can be achieved by coating these liposomes with targeting ligands which actively target specific receptors that are overly expressed on the membranes of the cancer cells [6]. This will ensure the specific delivery of the liposomal anticancer agents to the tumor site.

Human serum albumin (HSA) is a multi-functional protein that is able to bind and transport numerous endogenous and exogenous molecules [7]. When the cells are stressed, as is the case with the fast-growing cancer cells, albumin is taken up by cells as a source of amino acids and energy needed for cell proliferation [8]. Albumin represents a high percentage of the total amount of extracellular protein in tumor cytosol for patients suffering from breast cancer [9]. A number of studies have reported that albumin receptors (heterogeneous nuclear ribonucleoproteins-hnRNP) are localized on the surface of the cancer cells [10, 11]. In experimental animals bearing solid tumors, radioactively- or fluorescently labeled albumin was highly taken up by the tumor cells compared to the healthy cells [12] while Germain et al. [13] reported that albumin is internalized by human breast cancer cells (MDA-MB 231 and MCF-7) in culture, by using confocal laser scanning microscopy. Therefore, pegylated liposomes labeled with HSA are suitable targeting carriers to deliver therapeutic drugs to HSA receptors' overexpressing cancer cells due to their targeting capabilities, their colloidal stability, and long blood-circulation time [14].

Following the accumulation at the tumor site, liposomes show slow rate of release of the loaded drug [15, 16]. Therefore, it is important to apply smart triggering mechanisms that are strong enough to quickly and completely release the drug loaded inside these liposomes. There are a number of drug release triggering mechanisms which have been reported in the literature, such as pH, temperature, enzymes and UV-light stimuli [17, 18, 19, 20]. In recent years, ultrasound has been reported as one of the best drug release triggering techniques [21, 22]. This is due to the fact that it is a cost-limited non-invasive technique that allows focusing the beam precisely on the tumor. Ultrasound exposure of tumor tissue comprising sonosensitive liposomes may, not only, induce drug release from these carriers, but also increase intracellular drug uptake. Ultrasound consists of sound waves (acoustic waves) with a frequency higher than 20 kHz [23]. When the

ultrasound waves are traveling through a medium, a series of compression and rarefaction events occurs creating areas of high and low pressure, respectively. As the waves propagate in the medium, the particles of the medium oscillate in place forwards and backwards which mediates the progression of the waves [24]. Depending on frequency, intensity (or power density) and length of exposure time, the US waves can be focused on and absorbed by tissues in several ways, so as to achieve different effects for a specific purpose. The therapeutic effects of US are divided into thermal and non-thermal. The non-thermal or mechanical effect is known as the “acoustic cavitation” [22]. While the thermal effect is generally generated by high-intensity focused US (HIFU) in the continuous mode, the mechanical effects of ultrasound (cavitation) are predominantly generated from pulsed low-frequency ultrasound (LFUS).

In this study, the mechanical effect generated by pulsed low-frequency ultrasound at different densities will be used to trigger the release of the model drug “calcein” encapsulated in non-targeted and HSA-targeted liposomes. Calcein is a water-soluble self-quenching fluorescent dye, the relief of self-quenching is used as an indicator of calcein leakage from the encapsulating liposome. Ultrasound-mediated triggering of calcein release will result in enhancing calcein uptake by both breast cancer cell lines (MDA-MB-231 and MCF-7). In addition, LFUS generates transient or permanent pores in the walls of blood vessels at the tumor site (sonoporation) resulting in a significant enhancement of the extravascular delivery of therapeutics in the tumor site.

2. Materials and methods

2.1. Materials

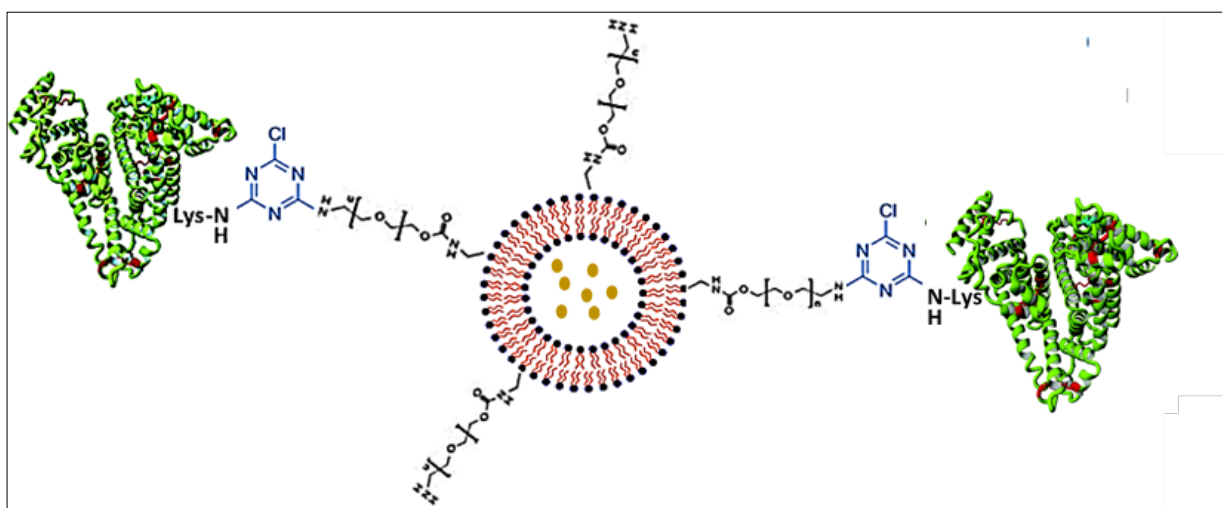
1,2-dipalmitoyl-sn-glycero-3-phosphocholine (DPPC) and 1,2-distearoyl-sn-glycero-3-phosphoethanolamine-N-[amino(polyethylene glycol)-2000] (DSPE-PEG(2000)-NH₂) were obtained from Avanti Polar Lipids Inc. (Alabaster, AL, USA). Human serum albumin (M_w = 68 KD), Calcein disodium salt, bicinchoninic acid (BCA) kit, chloroform, cholesterol, Sephadex® G-100 and 2,4,6 trichloro-1,3,5 triazine (cyanuric chloride) were obtained from Sigma-Aldrich (St. Louis, MO, US), supplied through LABCO LLC. Dubai, UAE). HeLa, MCF-7 and MDA-MB-231 cell lines were obtained from ECACC.

2.2. Preparation of non-targeted liposomes

The liposomes were prepared according to the modified lipid film hydration method described by Lasch *et al.* [25]. The lipids 1,2-dipalmitoyl-sn-glycero-3-phosphocholine (DPPC), 1,2-distearoyl-sn-glycero-3-phosphoethanolamine-N-[amino(polyethylene glycol)-2000] (DSPE-PEG(2000)-NH₂) and cholesterol at a molar ratio of 65:5:30, respectively, were dissolved in chloroform in a round bottom flask. A lipid film was formed by removing the chloroform using a rotatory evaporator at 50 °C for 15 mins. The film was then hydrated with 2 mL of 50 mM calcein (dissolved in phosphate buffer saline (PBS) and the pH adjusted to 7.4) using the rotatory evaporator (without applied vacuum) for 50 mins at 60 °C followed by sonication at 60 °C using a sonication bath (Agar Scientific) for 2 mins. The formed liposomes were then extruded at 60 °C through the 0.2 µm polycarbonate membrane using Avanti® mini-extruder (Avanti Polar Lipids, Inc., Alabaster, AL, USA). The liposomes were purified using Sephadex® G-100 gel filtration (size exclusion chromatography) prepared with borate buffer (pH~8.5). The purified liposomes were collected and stored at 4 °C until used.

2.3. Preparation of targeted liposomes

The covalent attachment of the liposomes to the lysine residues of HSA was carried out using cyanuric chloride (2,4,6 trichloro-1,3,5 triazine) as a coupling agent. Cyanuric chloride (CC) was reacted with the targeted liposomes at a 1:1 molar ratio with DSPE-PEG-NH₂ for 3 hours at 0 °C. A solution of HSA (50 µl) in Borate (pH~8.5) was then added drop wise to the liposomes (final concentration of 0.25 mg/mL) and the reaction was left to stir overnight at room temperature to allow the conjugation reaction to proceed. The un-reacted protein was then removed using Sephadex® G-100 gel filtration prepared with PBS buffer (pH~7.4).



2.4. Measuring the size of liposomes by Dynamic Light Scattering

The mean size of the liposomes was determined by Dynamic Light Scattering (DLS) using the DynaProVR NanoStar™ (Wyatt Technology Corp., Santa Barbara, CA, USA). The hydrodynamic radius (Rh) of the diluted liposomes (10 µl in 1 ml PBS) was determined at room temperature.

2.5. Estimation of phospholipid content using Stewart assay

The phospholipid content of the liposomes was determined colorimetrically using the Stewart assay. The prepared liposomes were transferred to a round bottom flask and were dried in the rotary evaporator under vacuum. Chloroform (1 mL) was added to the flask followed by sonication for 20 seconds. 200 μ l of the liposomes were then transferred a pyrex tube containing 1.8 mL chloroform. 2 ml of ammonium ferrothiocyanate was added, and the mixture was sonicated for 20 seconds followed by centrifugation 10 mins at 1000 rpm. The top dark layer was removed and discarded while the optical density of the bottom clear chloroform layer was measured using UV-VIS spectroscopy at $A_{\max}=485$ nm. Three replicates for each sample were used.

2.6. Protein quantitation using Bicinchoninic acid assay (BCA)

The colorimetric BCA Protein Assay was used to estimate protein content in HSA-PEG liposomes. The BCA reagent was prepared by mixing QuantiPro™ QA buffer: QuantiPro™ QB: CuSO_4 at a ratio of 25:25:1. 400 μ l of the liposomes were added to Eppendorf tube containing 600 μ l PBS buffer, 1 ml of the reagent were added, and the tubes were incubated 60 °C for 1 h. The absorbance of the samples were measured using UV-VIS spectroscopy at $A_{\max}=562$ nm. Three replicates for each sample were used.

2.7. Cell cultures

The MCF-7 and MDA-MB-231 breast cancer cell lines were cultured in RPMI medium supplemented with 10% heat-inactivated fetal bovine serum (FBS) and 1 % penicillin-streptomycin (Sigma- Aldrich, St Louis, MO, USA). The cultures were maintained at 37 °C in a humidified atmosphere with 5 % CO_2 . Cells were in the logarithmic growth phase by routine passage every 2–3 days and split when reaching confluence. For the cellular uptake of the

liposomes studies, exponentially growing cells were harvested with 3 ml of trypsin (0.25 % from Sigma-Aldrich) and 3×10^5 cell/mL of growth medium were seeded in 6-well plates to reach confluency at the time of the experiment.

2.8. The physical stability of the control and HSA-PEG Liposomes

Both non-targeted and the HSA-PEG liposomes were added to the RPMI medium supplemented with 10 % heat-inactivated fetal bovine serum (FBS) and were incubated at 37 °C for 24 hours. A comparison between calcein released from both types of liposomes was conducted using the QuantaMaster QM 30 Phosphorescence Spectrofluorometer (Photon Technology International, Edison NJ, USA). 50 μ l of 1 % (v/v) TX-100 was added to the sample cuvette to lyse the liposomes and release all the encapsulated calcein. The corresponding fluorescence intensity is characterized as 100 % release.

2.9. Low-Frequency ultrasound release studies (online experiments)

Low-frequency ultrasound (20-kHz) was used to trigger the release of calcein encapsulated in the liposomes. Calcein release was monitored by fluorescence changes using a QuantaMaster QM 30 Spectrofluorometer (Photon Technology International, Edison NJ, USA). Calcein is a fluorescent molecule with excitation and emission wavelengths of 495 nm and 515 nm respectively. To prepare the samples in the test cuvette, 75 μ l of the liposomes were diluted with 3 ml of the PBS buffer. The initial fluorescence (F_0) was recorded for the first 60 seconds without sonication to generate a baseline. The sonication was then applied using a 20-kHz ultrasonic probe (model VCX750, Sonics & Materials Inc., Newtown, CT) on a pulsed mode with 20 seconds “on” and 10 seconds “off” cycle for 4 minutes. This was followed by the addition of 50 μ l of 1 % (v/v) Triton

X-100 into the sample cuvette to lyse liposomes and release all the encapsulated calcein. The corresponding fluorescence intensity is characterized as 100 % release. The percentage of calcein release was then calculated at a given time using the fluorescence intensity values obtained experimentally according to the following equation,

$$\% \text{ Drug Release} = \frac{F - F_0}{F_{TX100} - F_0} \times 100 \quad (1)$$

Where F is the fluorescence intensity at the time (t) of insonation, F_0 is the average of the initial fluorescence intensity before exposing the sample to the US, and F_{TX-100} is the maximum fluorescence achieved after lysing liposomes.

2.10. Cellular uptake of the non-targeted and HSA-targeted liposomes

The breast cancer cell lines MDA-MB-231 and MCF-7 were incubated and sonicated with both the non-targeted and the HSA-PEG liposomes at a concentration of 200 μ M of DPPC. The liposomes were added to 6-well plates containing the cancer cell lines for 30 minutes in humidified air at 37 °C and 5 % CO₂. The plates were then washed with PBS buffer and harvested with a trypsin solution for analysis using flow cytometry measurements (Beckman Coulter FC500). As aforementioned, samples were analyzed to measure calcein fluorescence intensity utilizing an excitation and emission wavelengths of 495 nm and 515 nm, respectively. At least three independent assays were performed for each treatment.

2.11. Application of low-frequency ultrasound on cancer cells incubated with the control and HSA-PEG liposomes

To study the effect of the low-frequency ultrasound on the cellular uptake of liposomes, both the control and the HSA-PEG liposomes were incubated with MDA-MB-231 and MCF-7 breast cancer cell lines at the same previous conditions. After the initial 60 minutes of incubation, the plates were continuously sonicated floating in a 40-kHz with a density of 1 W/cm² (Branson 3510-DTH Ultrasonic Cleaner) for 5 minutes. No temperature increase was observed in cell-containing wells during the sonication. After ultrasound exposure, the plates were incubated for an hour in humidified air at 37 °C and 5 % CO₂. The plates were then washed with PBS buffer and harvested with trypsin solution for calcein uptake quantification using flow cytometry. In each insonation experiment, the sonolysis studies (the effect of US on cell viability) were performed using the Trypan blue exclusion assay, and the cell viabilities were always higher than 90 %.

2.12. Statistical analysis

The differences between the results were compared using a two-tailed t-test with the assumption of unequal variances. Two values were considered significantly different when $p \leq 0.05$.

3. Results

3.1. Preparation of HSA-PEG-conjugated liposomes

HSA-PEG-conjugated liposomes were prepared by the attachment of HSA to the PEG chain on the outside of the liposomes surface. Cyanuric chloride was used as a coupling agent linking the amino group (-NH₂) of the many accessible primary amino groups (lysine) on the surface of HSA to the amino group on the polyethylene glycol (PEG) chain of DSPE-PEG₍₂₀₀₀₎NH₂. Stewart and BCA assays were conducted to measure lipid content and confirm the attachment of the protein to the liposomes. The control sample for the assays was prepared by mixing a sample of the non-targeted liposomes with HSA without coupling agent cyanuric chloride. The mixture was then filtered through the size-exclusion gel, under similar conditions as that of HSA-PEG-conjugated liposomes. The Stewart assay showed that both the control and HSA-PEG-conjugated liposomes had no significant difference in their phospholipid concentration represented by the DPPC content showing values of (5.61 ± 0.18 mg/ml and 5.24 ± 0.73 mg/ml respectively, p=0.832). The protein content was significantly higher in the HSA-PEG-conjugated liposomes compared to the control liposomes showing on average a 3-fold increase in protein content (0.35 ± 0.006 µg/ml for the control liposomes and 1.05 ± 0.43 µg/ml for the HSA-PEG liposomes, p=0.0256) which confirms the conjugation of the HSA to the PEG liposomes.

3.2. The size of the synthesized liposomes

The radius of the non-targeted (control) liposomes was on average 84.46 ± 0.97 nm with a polydispersity index (PDI) of 7.21 ± 1.42. HSA-PEG liposomes showed an average size of 84.86 ± 1.81 with a PDI of 9.68 ± 0.94 (Figure 1). Therefore, both types of liposomes were unilamellar structures with no significant difference in size (p=0.934).

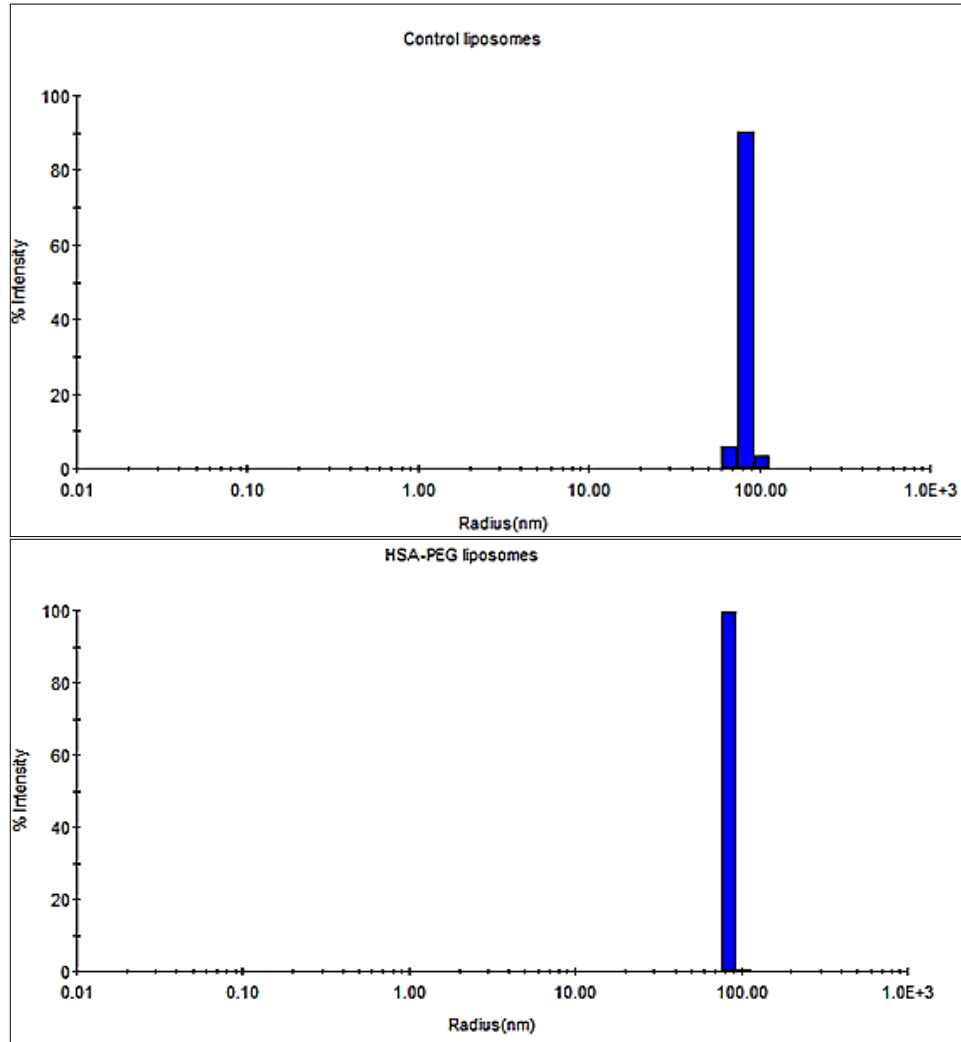


Figure 1. Size distributions of the non-targeted (control liposomes on the top and the HSA-PEG liposomes in the bottom).

3.3. *In vitro* release kinetics following insonation with LFUS

The rate and kinetics of drug release from the non-targeted (control) and HSA-PEG liposomes as a function of LFUS ultrasound exposure were evaluated using a frequency of 20 kHz in a pulsed mode (20 sec “on” and 10 sec “off”) for 4 minutes. In addition, the rate and kinetics of drug release were compared at three different power densities (6, 7 and 12 W/cm² respectively). The normalized-averaged release profiles of the non-targeted (control) and HSA-PEG liposomes are

shown in Figure 2. Lysing the liposomes using Triton-X-100 showed that both the control and HSA-PEG liposomes release most of their encapsulated calcein by 4 mins of the pulsed LFUS.

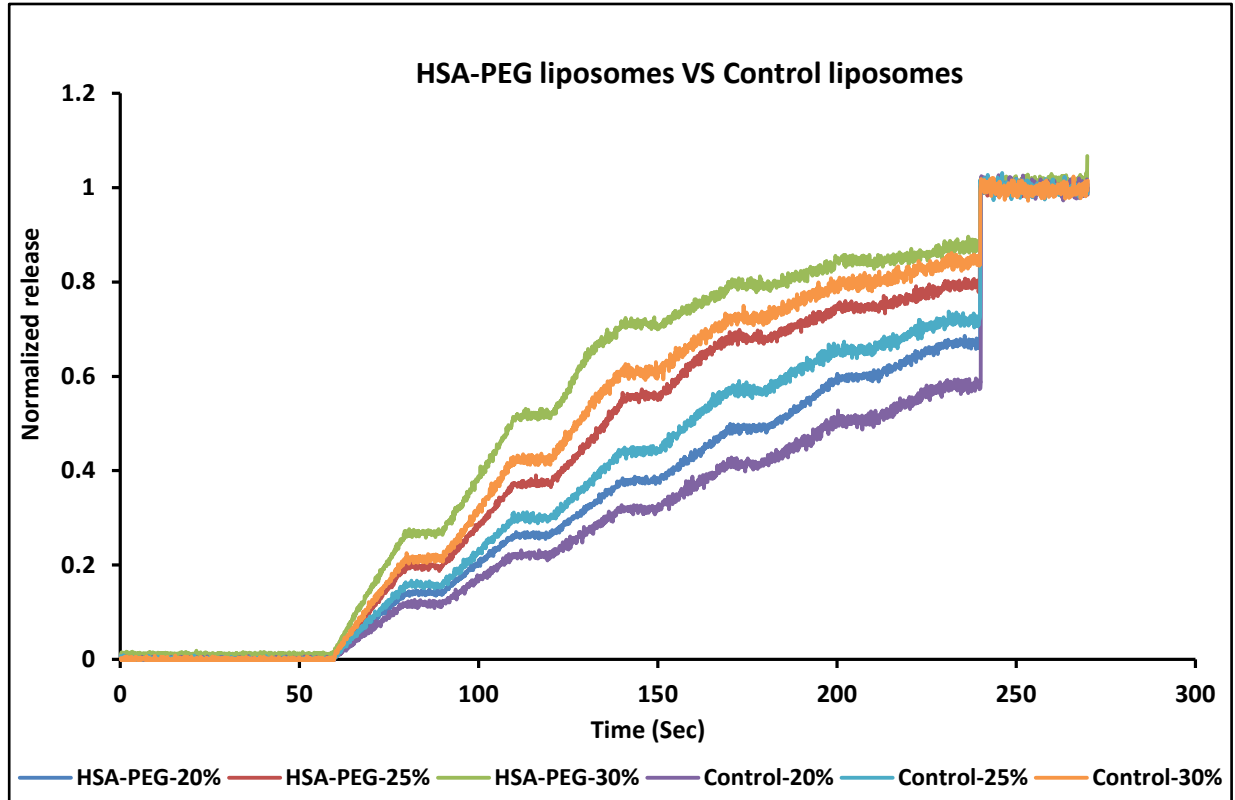


Figure 2. Normalized release profiles for non-targeted (control) and HSA-PEG liposomes triggered by pulsed 20-kHz LFUS for nearly 4 minutes at three power densities [20 % (6 w/cm^2), 25 % (7 w/cm^2) and 30 % (12 w/cm^2)].

As shown in Figure 3, the percentage of calcein release significantly increased with the increasing intensities during the first three pulses for both types of liposomes. Interestingly, the HSA-PEG liposomes showed a higher rate of calcein release compared to the non-targeted liposomes following the first ($p=0.003$), the second ($p=0.01$) and the third ($p=0.019$) pulses at the lowest power density used (6 W/cm^2). The same was observed with the higher power density of 7 W/cm^2 where HSA-PEG liposomes released more calcein compared to the non-targeted liposomes

following the first ($p=0.00007$), second ($p=0.0002$) and the third ($p=0.00002$) pulses. Furthermore, the similar pattern continued following the sonication using the highest power density (12 W/cm^2) where HSA-PEG liposomes released more calcein compared to the control following the first ($p=0.0003$), second ($p=0.0001$) and the third ($p=0.0001$) pulses. Overall, the highest percentage of calcein release was recorded with the highest intensity of 12 W/cm^2 (30%) following the third pulse releasing $60.86 \pm 7.1 \%$ of the calcein encapsulated in the control liposomes and $71.09 \pm 5.5 \%$ of the calcein encapsulated in the HSA-PEG liposomes. No significant change in the size of the liposomes was recorded following the first three pulses in all power densities tested here.

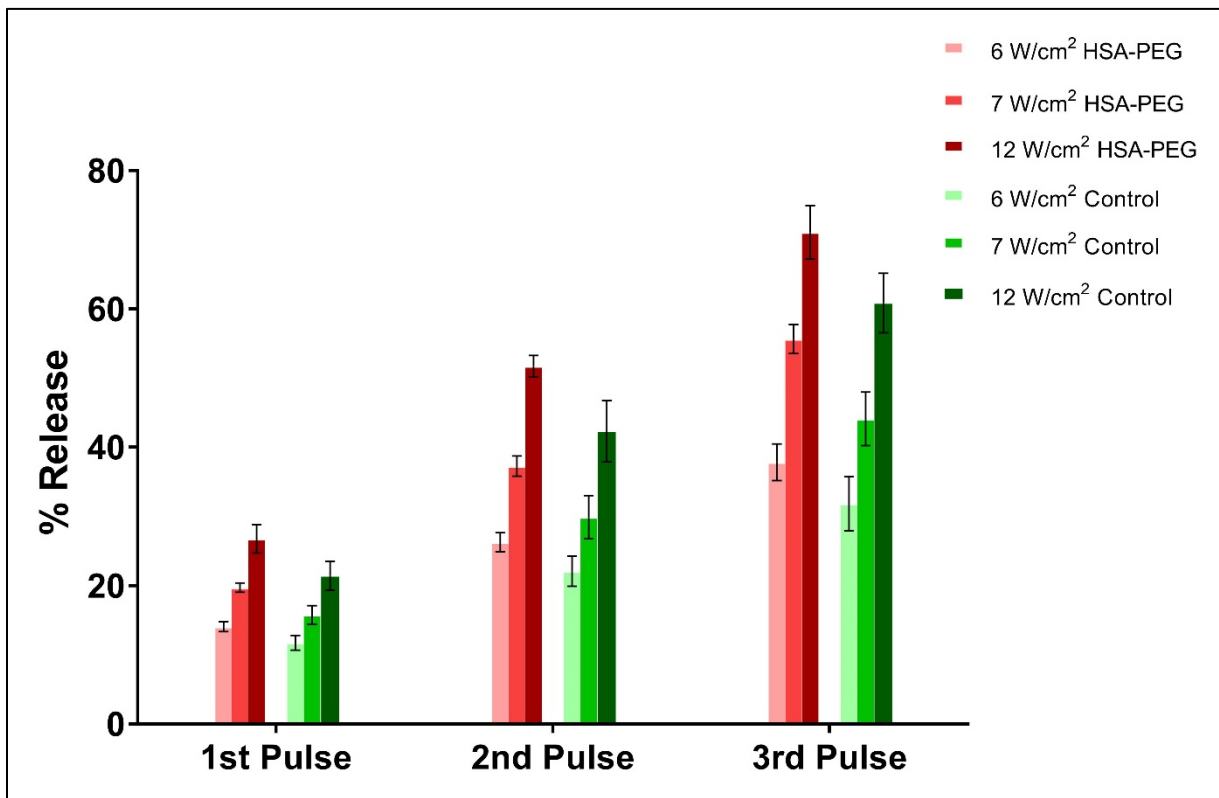


Figure 3. Percentage release of the calcein encapsulated inside the control and HSA-PEG liposomes following the first three pulses at different power densities (6 W/cm^2 , 7 W/cm^2 , and 12 W/cm^2).

3.4. Intracellular uptake and targeting potential of the HSA-PEG liposomes and the effect of low-frequency ultrasound

In this study, the subcellular internalization of the model drug calcein was evaluated by flow cytometry as shown in Figure 4. The mean fluorescent intensity (MFI) of the HSA-PEG liposomes was significantly higher than that of the control liposomes in both the MDA-MB-231 and MCF-7 breast cancer cell lines showing 84 % ($p= 0.0002$) and 90 % ($p= 0.0001$) increase in calcein uptake respectively when compared to the non-targeted control liposomes. Sonication of both breast cancer cell lines (MDA-MB-231 and MCF-7), previously incubated with the HSA-PEG liposomes, by floating in a 40-kHz water bath significantly increased the intracellular uptake of calcein by the MDA-MB-231 breast cancer cell line by 155 % compared to the control liposomes ($p = 0.0001$). The same was observed when the MCF-7 breast cancer cell line was sonication exhibiting a 175 % increase in calcein uptake ($p=0.0009$).

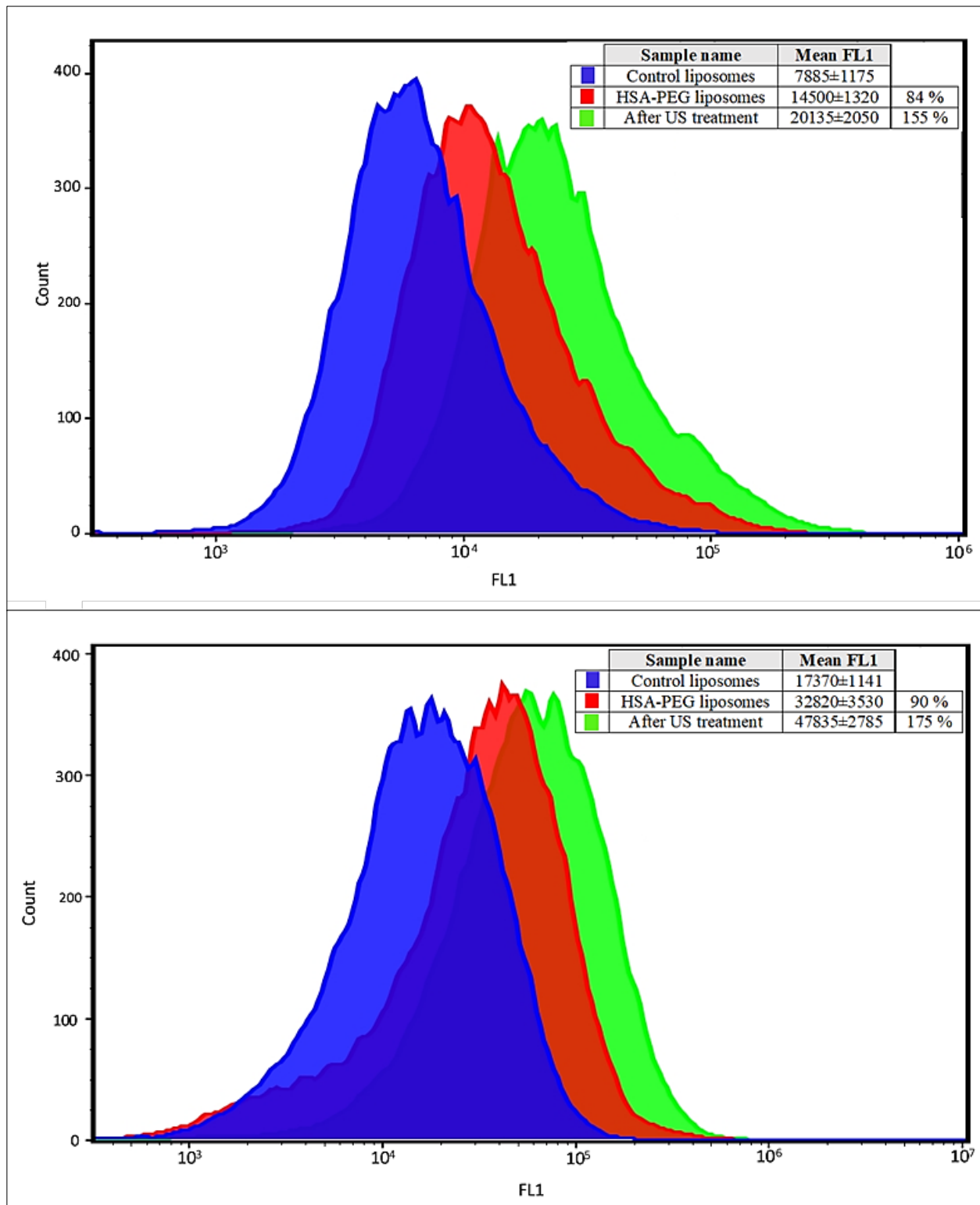


Figure 4. Enhanced Calcein uptake by the breast cancer cell lines MDA-MB-231 (top) and MCF-7 (bottom) following the incubation of these cells with HSA-PEG liposomes for 1 hour. Exposure to ultrasound (40 kHz for 5 mins) further enhanced calcein uptake by both cell lines. Results are average \pm standard deviation of three liposome batches (3 replicates each).

To confirm the specificity of albumin binding to the surface of the two breast cancer cell lines, the same experiment was conducted on the cervical cancer cell line “HeLa”. This cell line does not overexpress albumin receptors on its surface. Following the incubation of both the control and HSA-PEG liposomes with the HeLa cell line, the geometric means of the average cellular calcein uptake for control and the HSA-PEG liposomes were 2773 ± 110 and 2885 ± 435 , respectively (Figure 5). These values were not statistically different ($P = 0.074$) which indicated that the uptake of calcein in the HeLa cell line is not affected by the presence of the HSA on the surface of the liposomes. These findings show that the presence of the HSA receptors on the surfaces of the breast cancer cell lines MDA-MB-231 and MCF-7 could be utilized to effectively target cancer cells reducing the cytotoxicity and enhancing the efficacy of the encapsulated therapeutic drugs.

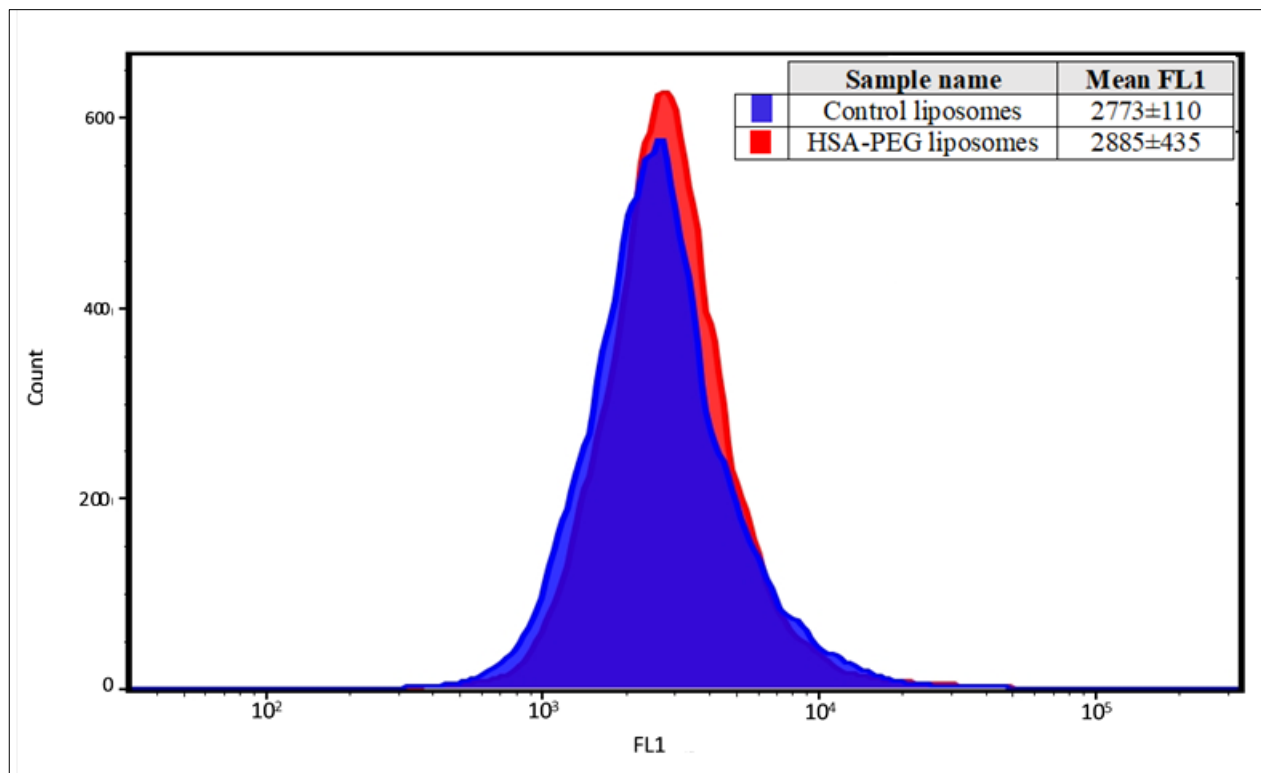


Figure 5. Calcein uptake by the cervical cancer cell line HeLa. No enhancement of calcein uptake was observed following the incubation of the cancer cells with HSA-PEG liposomes compared to the control liposomes. Results are average \pm standard deviation of three liposome batches (3 replicates each).

3.5. Physical stability of the control and HSA-PEG liposomes in fetal bovine serum medium

The stability of both the control and HSA-PEG liposomes incubated in fetal bovine serum medium following 1 h and 24 h incubation at 37 °C was analyzed by comparing the rate of calcein release from these liposomes. Triton X-100 was used to lyse the cells releasing 100 % of the encapsulated calcein. As shown in Figure 6, both the control and HSA-PEG liposomes showed no significant difference in the rate of releasing the encapsulated calcein following 1 h (control= 2.69 % ± 0.264; HSA-PEG= 3.35 % ± 0.183, P= 0.818) and 24 h (control= 13.29 % ± 0.303; HSA-PEG=14.94 % ± 0.272, P= 0.187) incubation. This result indicates that the higher uptake of calcein by the breast cancer cell line from HSA-PEG liposomes, compared to the control liposomes, is not due to the lower stability of the HSA-PEG liposomes.

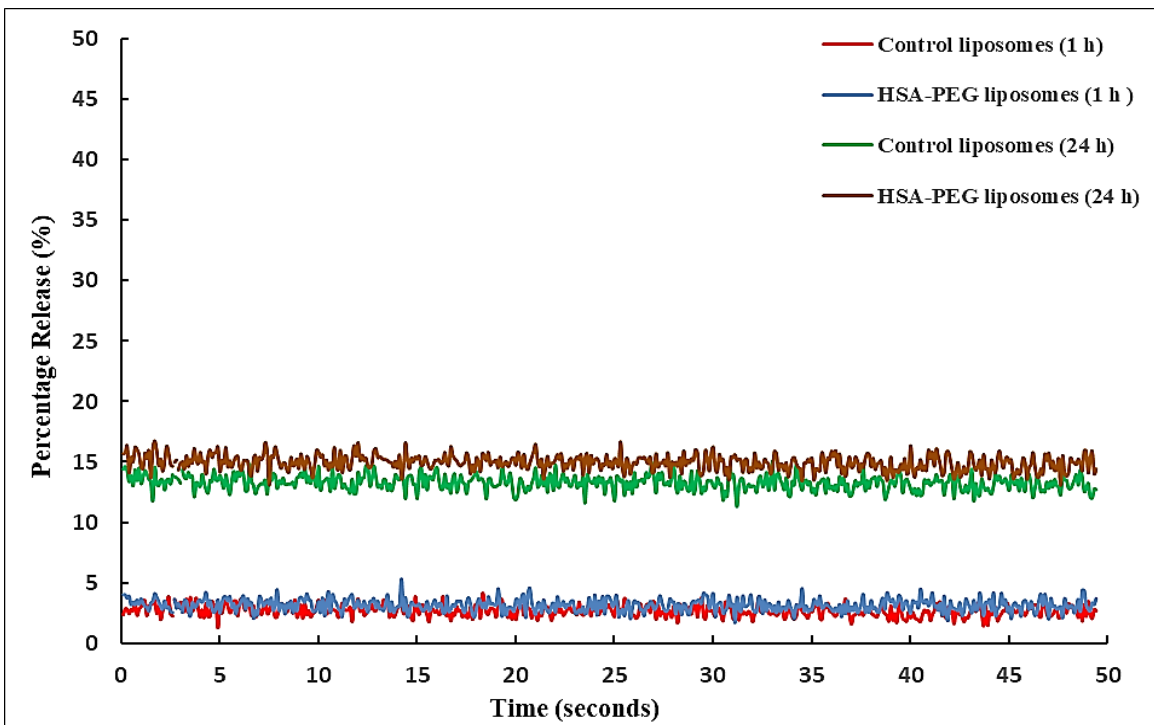


Figure 6. Control and the HSA-PEG liposomes showed a similar level of stability when incubated in fetal bovine serum medium at 37 °C for 1 h and 24 h. No significant difference was observed in the amount of calcein released during the incubation period. Results are the average of three liposome batches.

4. Discussion

This study investigated the effect of coupling human serum albumin into the surface of PEG-liposome triggered with LFUS on calcein uptake by the breast cancer cell lines MDA-MB-231 and MCF-7. Our data indicated that the synthesized pegylated liposomes loaded with the model drug calcein and conjugated to the human serum albumin (HSA) are stable at the physiological temperature in the presence of fetal bovine serum medium. These targeted liposomes released only 14.94 % of their load following 24 hours incubation, in fetal bovine serum medium, at 37 °C making them suitable for medical use as targeted drug carriers. Our results also showed that the synthesized liposomes were around 84.46 ± 0.97 nm in radius, HSA modification had an insignificant effect on the size of these liposomes showing a radius of (84.86 ± 1.81) nm. This is in agreement with Furumoto et al. [14] who reported that serum albumin attached to the surface of the liposomes that were around 200 nm in diameter had no significant effect on their size. Generally, the pore size of tumor microvessels varies from 100 to 1200 nm in diameter. This would allow the extravasation of these targeted liposomes into tumor tissue but not into normal tissue. Thus, increasing the efficiency while reducing the toxicity of the encapsulated drug.

We applied ultrasound as an external stimulus to trigger the release of the encapsulated calcein from both the non-targeted and the HSA-targeted liposomes. The liposomes were sonicated with LFUS at 20-kHz at different power densities. A number of studies have reported the use of LFUS to trigger the release of the drugs encapsulated inside other nanocarriers, such as polymeric micelles [26] and polymeric matrices [27] as well as to enhance the permeability of biological membranes for drug and gene delivery [28].

In this study, we reported that LFUS significantly enhanced calcein release from both the control and HSA-PEG liposomes. The highest power density used (12 W/cm^2) was the most sufficient to cause cavitation in the solution capable of releasing high percentages of the encapsulated calcein in both types of liposomes. This is in agreement with previous studies which showed that applying LFUS (20 kHz) triggers the release of the drugs encapsulated inside the liposomes in a controlled manner [21, 29, 30]. In addition, Cohen [31] showed that 20 kHz ultrasonic irradiation to be more efficient in drug release from liposomes than high-frequency ultrasound (1 and 3 MHz). This could be due to the fact that the intensity needed to induce transient cavitation is lower at low frequencies [32].

The enhanced calcein release triggered by LFUS reported here is mainly due to the mechanical effect (acoustic cavitation) of the ultrasound. However, the energy released from the cavitation process results in a temperature rise. During sonication of the liposomes using the ultrasound probe, we observed an increase in temperature following the end of the third pulse (from $25 \text{ }^\circ\text{C}$ to $32 \text{ }^\circ\text{C}$). This rise in temperature is still below the transition temperature (T_m) of the phospholipid DPPC ($41.3 \text{ }^\circ\text{C}$) but does not eliminate the role of the thermal effect of the temperature rise in enhancing the release. Previous studies have shown that ultrasonic absorbance by the lipid bilayer occurs during lipid phase transition, while the absorbance by the membrane is diminishing below the phase transition. This suggests that liposomal drug release, achieved when working below the phase transition temperature is attributed to mechanical and possible thermal effects due to the rise in temperature rather than absorbance of ultrasound by the lipid bilayer [33, 34].

We reported no change in the size of the liposomes following the first three pulses of ultrasound in all the power densities tested here suggesting a pore-mediated release mechanism rather than a full distraction of the bilayer membrane of the liposomes. This is in agreement with Evjen et al. [35] who reported that liposomes based on phosphatidylcholine showed evidence of pore-mediated release mechanisms. Earlier studies have shown that the presence of PEG on the surfaces of the liposomes was found to enhance the ability of low-frequency ultrasound (20 kHz) to permeabilize these liposomes [21, 29]. DSPE-PEG has a lower packing parameter (0.5), and higher critical aggregation concentration (CAC) of ($\sim 10^{-5}$ M) compared to the DPPC and other membrane lipids which have a higher packing parameter of 0.74-1.0 and a CAC value of $\sim 10^{-10}$ M. Therefore, DSPE-PEG is likely to be ejected out of the phospholipids bilayer to form micelles upon the exposure to ultrasound waves [29, 32, 36]. Our results showed that the conjugation of HSA to the surface of the liposomes resulted in enhancing their sonosensitivity. HSA-PEG liposomes significantly released more calcein in all the power densities used here compared to the control liposomes. A possible explanation for this observation is that the attachment of the HSA molecule to DSPE-PEG has further weakened the packing parameter of the DSPE-PEG. Thus, enhancing the ejection of the DSPE-PEG from the liposomal membrane resulting in the enhanced calcein release.

To internalize molecules from outside the cell, cells use a process called endocytosis. Via this process, cells can take up macromolecules, proteins and ligands [37]. The main endocytic routes are the clathrin-mediated endocytosis and the caveolae-mediated endocytosis. Caveolae are specialized membrane domains enriched in certain lipids cholesterol and proteins [38]. Caveolae can mediate endocytosis through a receptor-dependent or -independent fashion [39]. Caveolin-1 (Cav-1) is one of the main functional components of caveolae and plays an important role in

caveolae formation. It is expected that to induce tumor formation, rapid proliferation is required, and therefore downregulation of caveolin-1 expression may be necessary. The level of caveolin-1 is related to the invasiveness of the tumor [40]. According to Chatterjee et al. [41], nanoparticle conjugate of paclitaxel to human serum albumin exhibits efficacy in pancreatic cancer, non-small cell lung cancer and breast cancer. The study found that Cav-1 protein levels correlated positively with cancer sensitivity to their albumin base nanoparticles and therefore, caveolae are essential for the cancer uptake of albumin. In general, albumin binds to a cell-surface, 60-kDa glycoprotein (gp60) receptor (albondin). gp60 is localized in the caveolae and binds to caveolin-1 (an intracellular protein) with subsequent formation of the caveolae [42, 43].

A study by Voigt et al. [44] compared the uptake of the proteins bovine serum albumin (BSA) and transferrin between the HeLa cells and the human umbilical vein endothelial cells (HUVECs) using fluorescently labeled BSA which is known as markers for caveolae-mediated endocytosis and transferrin for clathrin-mediated endocytosis. These researchers found that although HeLa cells internalize more transferrin than HUVECs by three folds, a much stronger distinction in the uptake behavior of BSA which was 32-fold higher in HUVECs in comparison with HeLa cells. This is in agreement with the Sharma et al. [45] who reported that HeLa cells have low levels of Cav-1. A similar observation was recorded in this study where only breast cancer cell lines showed increased uptake of calcein from the HSA-PEG liposomes. Thus, we can conclude the coating of the pegylated liposomes with HSA enhances the uptake of the drug encapsulated inside these liposomes. This is due to the presence of the caveolae which is not the main route of endocytosis in the HeLa cells.

Sonoporation effect of the LFUS is more likely to be the mechanism behind the enhanced calcein uptake by both breast cancer cell lines reported here. Sonoporation will both improve cellular

uptake of the liposomes as well as enhancing the release of the encapsulated calcein by rupturing the liposomes which contain similar membranes to that of the cells. Some studies have investigated the changes in cell morphology immediately after the exposure to acoustic cavitation and reported the formation of pores in the membrane [46, 47]. In addition, other studies suggested that, following the exposure to LFUS, the levels of cellular uptake of calcein may be consistent with the levels of the pores formed in the membrane of these cells [48, 49]. In a recent work published by our group [50], we reported that the exposure of the estrone-positive breast cancer cell line (MCF-7) incubated with estrone-conjugated liposomes to low-frequency ultrasound revealed a statistically significant uptake of calcein compared to uptake without ultrasound. In this study, we report that no increase in the temperature was recorded during sonication suggesting that the mechanical effect of the LFUS led to the enhanced calcein uptake rather than the thermal effect. Furthermore, both the control and the HSA-PEG liposomes showed similar stability levels indicating that the higher uptake of calcein by the breast cancer cell line from HSA-PEG liposomes, compared to the control liposomes, is not due to the lower stability of the HSA-PEG liposomes. While this study is important as a proof of concept since it is an *in vitro* study in the absence of the circulation with blood, future work should include *in vivo* breast tumor models to determine the ultimate therapeutic efficacy of this platform.

5. Conclusion

In summary, the present study indicated that the HSA modification of pegylated liposome significantly enhanced their binding to the surface of the breast cancer cell line MDA-MB-231 and MCF-7, resulting in the enhanced uptake of the drug by cancer cells. The mechanical force

produced via the ultrasound waves enhanced cellular uptake of the liposomes and triggered calcein release from the nanocarriers, thus further enhancing the calcein uptake by the cancer cells. Thus, our HSA-coated liposome coupled with ultrasound-mediated triggered drug release holds attractivet potential in breast cancer chemotherapy.

Disclosure statement

No potential conflict of interest was reported by the authors.

Funding

This work was financially supported by the American University of Sharjah Faculty Research Grants, Al-Jalila Foundation (AJF 2015555), Al Qasimi Foundation, Patient's Friends Committee-Sharjah, and Dana Gas Endowed Chair for Chemical Engineering.

References

1. McKnight JA. Principles of chemotherapy. *Clinical Techniques in Small Animal Practice*. 2003 2003/05/01/;18(2):67-72. doi: <https://doi.org/10.1053/svms.2003.36617>.
2. Immordino ML, Dosio F, Cattel L. Stealth liposomes: review of the basic science, rationale, and clinical applications, existing and potential. *Int J Nanomedicine*. 2006;1(3):297-315. PubMed PMID: 17717971; PubMed Central PMCID: PMCPMC2426795. eng.
3. Bhushan B, Khanadeev V, Khlebtsov B, et al. Impact of albumin based approaches in nanomedicine: Imaging, targeting and drug delivery. *Adv Colloid Interface Sci*. 2017 Aug;246:13-39. doi: 10.1016/j.cis.2017.06.012. PubMed PMID: 28716187; eng.
4. Maeda H, Wu J, Sawa T, et al. Tumor vascular permeability and the EPR effect in macromolecular therapeutics: a review. *J Control Release*. 2000 Mar 1;65(1-2):271-84. PubMed PMID: 10699287; eng.
5. Cattel L, Ceruti M, Dosio F. From conventional to stealth liposomes: a new frontier in cancer chemotherapy. *Tumori*. 2003 May-Jun;89(3):237-49. PubMed PMID: 12908776; eng.
6. Hu CM, Kaushal S, Tran Cao HS, et al. Half-antibody functionalized lipid-polymer hybrid nanoparticles for targeted drug delivery to carcinoembryonic antigen presenting pancreatic cancer cells. *Mol Pharm*. 2010 Jun 7;7(3):914-20. doi: 10.1021/mp900316a. PubMed PMID: 20394436; PubMed Central PMCID: PMCPMC2884057. eng.
7. Merlot AM, Kalinowski DS, Richardson DR. Unraveling the mysteries of serum albumin-more than just a serum protein. *Front Physiol*. 2014;5:299. doi: 10.3389/fphys.2014.00299. PubMed PMID: 25161624; PubMed Central PMCID: PMCPMC4129365. eng.
8. Stehle G, Sinn H, Wunder A, et al. Plasma protein (albumin) catabolism by the tumor itself--implications for tumor metabolism and the genesis of cachexia. *Crit Rev Oncol Hematol*. 1997 Jul;26(2):77-100. PubMed PMID: 9298326; eng.
9. Soreide JA, Lea OA, Kvinnsland S. Cytosol protein content and prognosis in operable breast cancer. Correlations with steroid hormone receptors and other prognostic factors. *Breast Cancer Res Treat*. 1991 Dec;20(1):25-32. PubMed PMID: 1813067; eng.
10. Satoh H, Kamma H, Ishikawa H, et al. Expression of hnRNP A2/B1 proteins in human cancer cell lines. *Int J Oncol*. 2000 Apr;16(4):763-7. PubMed PMID: 10717246; eng.
11. Sueoka E, Goto Y, Sueoka N, et al. Heterogeneous nuclear ribonucleoprotein B1 as a new marker of early detection for human lung cancers. *Cancer Res*. 1999 Apr 1;59(7):1404-7. PubMed PMID: 10197602; eng.
12. Stehle G, Sinn H, Wunder A, et al. The loading rate determines tumor targeting properties of methotrexate-albumin conjugates in rats. *Anticancer Drugs*. 1997 Aug;8(7):677-85. PubMed PMID: 9311444; eng.
13. Germain P, Metezeau P, Hellio R, et al. Internalization and biological effects of serum albumin in the breast cancer MCF-7 and MDA-MB 231 cells. *Cell Mol Biol (Noisy-le-grand)*. 1995 Dec;41(8):1119-29. PubMed PMID: 8747093; eng.
14. Furumoto K, Yokoe J, Ogawara K, et al. Effect of coupling of albumin onto surface of PEG liposome on its in vivo disposition. *Int J Pharm*. 2007 Feb 1;329(1-2):110-6. doi: 10.1016/j.ijpharm.2006.08.026. PubMed PMID: 17000067; eng.
15. Manzoor AA, Lindner LH, Landon CD, et al. Overcoming limitations in nanoparticle drug delivery: triggered, intravascular release to improve drug penetration into tumors. *Cancer Res*. 2012 Nov 1;72(21):5566-75. doi: 10.1158/0008-5472.can-12-1683. PubMed PMID: 22952218; PubMed Central PMCID: PMCPMC3517817. eng.

16. El-Kareh AW, Secomb TW. A Mathematical Model for Comparison of Bolus Injection, Continuous Infusion, and Liposomal Delivery of Doxorubicin to Tumor Cells. *Neoplasia* (New York, NY). 2000 12/30/received 02/11/accepted;2(4):325-338. PubMed PMID: PMC1550297.
17. Turk MJ, Reddy JA, Chmielewski JA, et al. Characterization of a novel pH-sensitive peptide that enhances drug release from folate-targeted liposomes at endosomal pHs. *Biochim Biophys Acta*. 2002 Feb 10;1559(1):56-68. PubMed PMID: 11825588; eng.
18. O'Brien DF, Whitesides TH, Klingbiel RT. The photopolymerization of lipid-diacetylenes in bimolecular-layer membranes. *Journal of Polymer Science: Polymer Letters Edition*. 1981 1981/03/01;19(3):95-101. doi: 10.1002/pol.1981.130190302.
19. Zhu L, Kate P, Torchilin VP. Matrix metalloprotease 2-responsive multifunctional liposomal nanocarrier for enhanced tumor targeting. *ACS Nano*. 2012 Apr 24;6(4):3491-8. doi: 10.1021/nn300524f. PubMed PMID: 22409425; PubMed Central PMCID: PMC3337349. eng.
20. Needham D, Anyarambhatla G, Kong G, et al. A new temperature-sensitive liposome for use with mild hyperthermia: characterization and testing in a human tumor xenograft model. *Cancer Res*. 2000 Mar 1;60(5):1197-201. PubMed PMID: 10728674; eng.
21. Lin H-Y, Thomas JL. PEG-Lipids and Oligo(ethylene glycol) Surfactants Enhance the Ultrasonic Permeabilizability of Liposomes. *Langmuir*. 2003 2003/02/18;19(4):1098-1105. doi: 10.1021/la026604t.
22. Ahmed SE, Awad N, Paul V, et al. Improving the Efficacy of Anticancer Drugs via Encapsulation and Acoustic Release. *Curr Top Med Chem*. 2018;18(10):857-880. doi: 10.2174/1568026618666180608125344. PubMed PMID: 29886831; eng.
23. Evjen TJ, Nilssen EA, Rognvaldsson S, et al. Distearoylphosphatidylethanolamine-based liposomes for ultrasound-mediated drug delivery. *Eur J Pharm Biopharm*. 2010 Aug;75(3):327-33. doi: 10.1016/j.ejpb.2010.04.012. PubMed PMID: 20434558; eng.
24. Moussa HG, Martins AM, Hussein GA. Review on triggered liposomal drug delivery with a focus on ultrasound. *Curr Cancer Drug Targets*. 2015;15(4):282-313. PubMed PMID: 25760762; eng.
25. Lasch J, Weissig V, Brandl M. Preparation of liposomes. In: Torchilin VP, Weissig V, editors. *Liposomes—A Practical Approach*. 2nd ed: Oxford University Press; 2003. p. 3 – 30 . .
26. Hussein GA, Christensen DA, Rapoport NY, et al. Ultrasonic release of doxorubicin from Pluronic P105 micelles stabilized with an interpenetrating network of N,N-diethylacrylamide. *J Control Release*. 2002 Oct 4;83(2):303-5. PubMed PMID: 12363455; eng.
27. Kost J, Leong K, Langer R. Ultrasound-enhanced polymer degradation and release of incorporated substances. *Proc Natl Acad Sci U S A*. 1989 Oct;86(20):7663-6. PubMed PMID: 2813349; PubMed Central PMCID: PMC298130. eng.
28. Kinoshita M, Hynynen K. A novel method for the intracellular delivery of siRNA using microbubble-enhanced focused ultrasound. *Biochem Biophys Res Commun*. 2005 Sep 23;335(2):393-9. doi: 10.1016/j.bbrc.2005.07.101. PubMed PMID: 16081042; eng.
29. Schroeder A, Avnir Y, Weisman S, et al. Controlling liposomal drug release with low frequency ultrasound: mechanism and feasibility. *Langmuir*. 2007 Mar 27;23(7):4019-25. doi: 10.1021/la0631668. PubMed PMID: 17319706; eng.
30. Delalande A, Kotopoulis S, Postema M, et al. Sonoporation: mechanistic insights and ongoing challenges for gene transfer. *Gene*. 2013 Aug 10;525(2):191-9. doi: 10.1016/j.gene.2013.03.095. PubMed PMID: 23566843; eng.
31. Levi C. Ultrasound for targeted delivery of cytotoxic drugs from liposomes [M.Sc. Thesis]. Beer Sheva, Israel: Ben Gurion University; 2000.

32. Schroeder A, Kost J, Barenholz Y. Ultrasound, liposomes, and drug delivery: principles for using ultrasound to control the release of drugs from liposomes. *Chem Phys Lipids*. 2009 Nov;162(1-2):1-16. doi: 10.1016/j.chemphyslip.2009.08.003. PubMed PMID: 19703435; eng.
33. M. Maynard V, Magin R, R. Strom-Jensen P, et al. *Ultrasonic Absorption by Liposomes*. Vol. 2. 1983.
34. Tata DB, Dunn F. Interaction of ultrasound and model membrane systems: analyses and predictions. *The Journal of Physical Chemistry*. 1992 1992/04/01;96(8):3548-3555. doi: 10.1021/j100187a067.
35. Evjen TJ, Hupfeld S, Barnert S, et al. Physicochemical characterization of liposomes after ultrasound exposure - mechanisms of drug release. *J Pharm Biomed Anal*. 2013 May 5;78-79:118-22. doi: 10.1016/j.jpba.2013.01.043. PubMed PMID: 23474811; eng.
36. Ickenstein LM, Arfvidsson MC, Needham D, et al. Disc formation in cholesterol-free liposomes during phase transition. *Biochimica et Biophysica Acta (BBA) - Biomembranes*. 2003 2003/08/07/;1614(2):135-138. doi: [https://doi.org/10.1016/S0005-2736\(03\)00196-2](https://doi.org/10.1016/S0005-2736(03)00196-2).
37. Im J, K. Maiti K, Kim W, et al. Cellular Uptake Properties of the Complex Derived from Quantum Dots and G8 Molecular Transporter. Vol. 32. 2011.
38. Kumari S, Mg S, Mayor S. Endocytosis unplugged: multiple ways to enter the cell. *Cell Res*. 2010 Mar;20(3):256-75. doi: 10.1038/cr.2010.19. PubMed PMID: 20125123; eng.
39. Parton RG, Simons K. The multiple faces of caveolae. *Nat Rev Mol Cell Biol*. 2007 Mar;8(3):185-94. doi: 10.1038/nrm2122. PubMed PMID: 17318224; eng.
40. Cokakli M, Erdal E, Nart D, et al. Differential expression of Caveolin-1 in hepatocellular carcinoma: correlation with differentiation state, motility and invasion. *BMC Cancer*. 2009 02/24 08/19/received 02/24/accepted;9:65-65. doi: 10.1186/1471-2407-9-65. PubMed PMID: PMC2656543.
41. Chatterjee M, Ben-Josef E, Robb R, et al. Caveolae-Mediated Endocytosis Is Critical for Albumin Cellular Uptake and Response to Albumin-Bound Chemotherapy. *Cancer Res*. 2017 Nov 1;77(21):5925-5937. doi: 10.1158/0008-5472.can-17-0604. PubMed PMID: 28923854; PubMed Central PMCID: PMC5668166. eng.
42. John TA, Vogel SM, Tiruppathi C, et al. Quantitative analysis of albumin uptake and transport in the rat microvessel endothelial monolayer. *Am J Physiol Lung Cell Mol Physiol*. 2003 Jan;284(1):L187-96. doi: 10.1152/ajplung.00152.2002. PubMed PMID: 12471015; eng.
43. Jiang Y, Wong S, Chen F, et al. Influencing Selectivity to Cancer Cells with Mixed Nanoparticles Prepared from Albumin-Polymer Conjugates and Block Copolymers. *Bioconjugate Chemistry*. 2017 2017/04/19;28(4):979-985. doi: 10.1021/acs.bioconjchem.6b00698.
44. Voigt J, Christensen J, Shastri VP. Differential uptake of nanoparticles by endothelial cells through polyelectrolytes with affinity for caveolae [10.1073/pnas.1322356111]. *Proceedings of the National Academy of Sciences*. 2014;111(8):2942.
45. Sharma DK, Brown JC, Choudhury A, et al. Selective Stimulation of Caveolar Endocytosis by Glycosphingolipids and Cholesterol. *Molecular Biology of the Cell*. 2004 03/08/received 04/15/revised04/16/accepted;15(7):3114-3122. doi: 10.1091/mbc.E04-03-0189. PubMed PMID: PMC452569.
46. Tachibana K, Uchida T, Ogawa K, et al. Induction of cell-membrane porosity by ultrasound. *Lancet*. Vol. 353. England1999. p. 1409.
47. Jelenc J, Miklavčič D, Lebar AM, editors. Low-frequency ultrasound in vitro: Experimental system and ultrasound-induced changes of cell morphology. 2013 36th International Convention on

- Information and Communication Technology, Electronics and Microelectronics (MIPRO); 2013 20-24 May 2013.
48. Zarnitsyn V, Rostad CA, Prausnitz MR. Modeling transmembrane transport through cell membrane wounds created by acoustic cavitation. *Biophys J*. 2008 Nov 1;95(9):4124-38. doi: 10.1529/biophysj.108.131664. PubMed PMID: 18676653; PubMed Central PMCID: PMC2567961. eng.
 49. Zhang JZ, Saggar JK, Zhou ZL, et al. Different effects of sonoporation on cell morphology and viability. *Bosn J Basic Med Sci*. 2012 May;12(2):64-8. doi: 10.17305/bjbms.2012.2497. PubMed PMID: 22642588; PubMed Central PMCID: PMC4362440. eng.
 50. Salkho NM, Paul V, Kawak P, et al. Ultrasonically controlled estrone-modified liposomes for estrogen-positive breast cancer therapy. *Artif Cells Nanomed Biotechnol*. 2018 Apr 12:1-11. doi: 10.1080/21691401.2018.1459634. PubMed PMID: 29644867; eng.